Josephson Junctions and NEGF

Utkarsh[1,*]

[1] *Department of Electrical Engineering, Indian Institute of Technology Bombay, Powai, Mumbai-400076, India*

(Dated: October 31, 2023)

Josephson junctions are important components in superconducting electronics and are used in a variety of applications including quantum computing, magnetic field sensing, and microwave generation. Simulating the behavior of these junctions is crucial for understanding their performance and optimizing their design. The Non-Equilibrium Green's Function (NEGF) approach is a powerful technique for simulating the behavior of these junctions, taking into account both the quantum mechanical nature of the devices and the non-equilibrium conditions that arise in their operation. In this abstract, we present an overview of Josephson junctions and their importance in superconducting electronics, and discuss the use of the NEGF approach for simulating their behavior.

I. INTRODUCTION

A. BdG Equation - Andreev Reflection

For normal conductors, the electronic states are based on the Schrodinger equation. In the presence of superconductors, we need to use the Bogoliubov-de Gennes (BdG) equation to study the electronic states, as we will describe in this section.

Andreev Reflection: In Andreev reflection, on the other hand, an incident up-spin electron with energy E "drags" a down-spin electron with energy 2Ef - E along with it into the su perconductor. This leaves behind an empty state in the down-spin band that flows away from the interface. To describe Andreev reflection, we need to couple an up-spin electron with energy E to a down-spin hole with energy - (2Ef - E). This is accomplished by the following equation :

$$\left[\begin{array}{cc} \mathrm{H} & \Delta \mathrm{e}^{-\mathrm{i_f f_f}/\hbar} \\ \Delta^{*} \mathrm{e}^{+\mathrm{i}2\mathrm{E_f t}/\hbar} & -\mathrm{H}^{*} \end{array}\right]\left\{\begin{array}{c} \mathrm{u}' \\ \mathrm{v}' \end{array}\right\}=\mathrm{i}\hbar \frac{\partial}{\partial \mathrm{t}}\left\{\begin{array}{c} \mathrm{u}' \\ \mathrm{v}' \end{array}\right\} \tag{1}$$

The pairing potential $\mathrm{Ae}^{-\mathrm{i}2\mathrm{E_f t}/\hbar}$ provides the coupling necessary for Andreev reflection. The time-dependence $\mathrm{e}^{-\mathrm{i}2\mathrm{E_f t} t\hbar}$ is needed to cause the change in energy from E to $\mathrm{E}-2\mathrm{E_f}$.

Gauge Transformation:

$$\mathrm{u}=\mathrm{u}' \mathrm{e}^{+\mathrm{iE_f t}/\hbar} \quad \text{and} \quad \mathrm{v}=\mathrm{v}' \mathrm{e}^{-\mathrm{iE_f t}/\hbar} \tag{2}$$

gives the following BdG equation:

$$\left[\begin{array}{cc} \mathrm{H}-\mathrm{E_f} & \Delta \\ \Delta^{*} & -\left(\mathrm{H}^{*}-\mathrm{E_f}\right) \end{array}\right]\left\{\begin{array}{c} \mathrm{u} \\ \mathrm{v} \end{array}\right\}=\mathrm{i}\hbar \frac{\partial}{\partial \mathrm{t}}\left\{\begin{array}{c} \mathrm{u} \\ \mathrm{v} \end{array}\right\} \tag{3}$$

Non-equilibrium BdG has the following form:

$$\left[\begin{array}{cc} (\mathrm{H}-\mathrm{E_f}) & \Delta \mathrm{e}^{-\mathrm{i}2\mu(\mathrm{r})\mathrm{t}/\hbar} \\ \Delta^{*} \mathrm{e}^{+\mathrm{i}2\mu(\mathrm{r})\mathrm{t}/\hbar} & -\left(\mathrm{H}^{*}-\mathrm{E_f}\right) \end{array}\right]\left\{\begin{array}{c} \mathrm{u} \\ \mathrm{v} \end{array}\right\}=\mathrm{i}\hbar \frac{\partial}{\partial \mathrm{t}}\left\{\begin{array}{c} \mathrm{u} \\ \mathrm{v} \end{array}\right\} \tag{4}$$

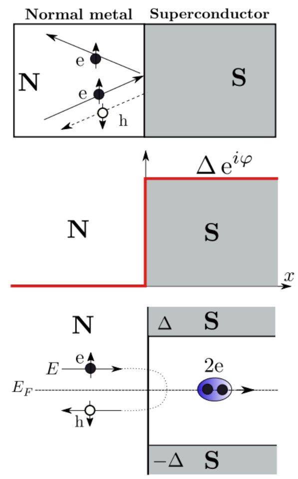

Figure 1: Normal v/s Andreev Reflection

1. *Particle-Hole Symmetry*

The BdG Hamiltonian in a given basis may be represented as a 2×2 matrix eigenvalue problem

$$E_M\left\{\begin{array}{c} u_m \\ v_m \end{array}\right\}=\left(\begin{array}{cc} \epsilon_m-E_f & \Delta \\ \Delta^* & -\left(\epsilon_m-E_f\right) \end{array}\right)\left\{\begin{array}{c} u_m \\ v_m \end{array}\right\},$$

diagonalized via the Bogoliubov-Valatin transformation $\gamma_m^{\dagger}=u_m c_{m,\uparrow}^{\dagger}+v_m c_{m \cdot \downarrow}$, representing the fact that the eigenstate is indeed a mixture of an up-spin electron and a down-spin hole. This yields two eigenvalues $E_m= \pm \sqrt{\left(\left(\epsilon_m-E_f\right)^2+|\Delta|^2\right.}$ symmetrically around $E=0$. In the second quantized form, we may write the mean field Hamiltonian as $H_{mf}=H_{Vac}+\sum_m E_m \gamma_m^{\dagger} \gamma_m$, which can also be re-written in the "ground state + excitation" picture as $H_{mf}=H_G+\sum_{E_m>0} E_m\left[\gamma_{m,\uparrow}^{\dagger} \gamma_{m,\uparrow}+\gamma_{m,\downarrow}^{\dagger} \gamma_{m,\downarrow}\right]$

Due to PH Symmetry the expectation values are given by:

$$<A>=2\left[\sum_{E_m>0} f_m<u_m\left|\hat{A}_{op}\right| u_m>+\right.$$

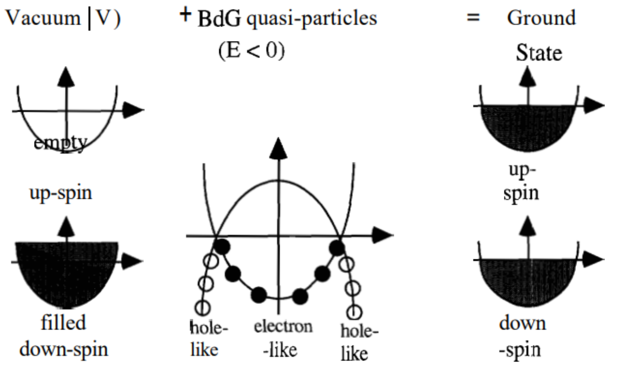

Figure 2: In a regular conductor, the lowest energy state can be achieved by populating all negative energy states of the **BdG** equation ($A = 0$), beginning with the unique vacuum state $|V\rangle$. This vacuum state contains a complete band of electrons with down-spin. The quasi-particles, which behave like electrons, fill the unoccupied band with up-spin, while the quasi-holes, which behave like positively charged particles, extend to negative infinity and empty out the filled band with down-spin. This results in the standard ground state where both bands are filled up to K = 0.

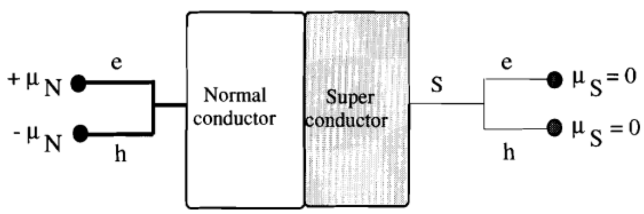

Figure 3: Multi-terminal model used to study N-S junction

$\sum_{E_m>0} (1 - f_m) < v_m \left| \hat{A}^*_{op} \right| v_m >$ (5)

B. NS Junction

It is possible to divide each physical lead (designated as i) into two parts, an electron-like and a hole-like lead, with potentials of μ_i respectively. This division allows us to calculate the current flowing across the N-S junction. Figure 3 depicts the normal terminal as being divided into two segments, while the superconducting contact is maintained at µS = 0 for both the electron-like and hole-like particles through an appropriate gauge transformation. Using this configuration, we can employ the Landauer multi-terminal formula to calculate the currents at the terminal.

$$I_i = \frac{e}{h} \int dE \sum_j [M_i \delta_{ij} - T_{ij} f_0 (E - \mu_j)$$

$$I_{Ne} = \frac{e}{h} \int dE \{[M_{Ne} - T_{Ne,Ne}] f_0 (E - \mu_N) + [-T_{Ne,Nh}] f_0 (E + \mu_N) + [-T_{N2,Se}] f_0(E) + [-T_{Ne,Sh}] f_0(E)$$

Making use of the sum-rule, i.e., $M_{Ne} = T_{Ne,Ne} + T_{Ne,Nh} + T_{Ne,Se} + T_{Ne,Sh}$, we obtain

$$I_{Ne} = \frac{e}{h} \int dE \{[M_{Ne} - T_{Ne,Ne}] [f_0 (E - \mu_N) - f_0(E)] + [-T_{Ne,Nh}]$$

Similarly, the current at the "Nh" terminal may be written as

$$I_{Nh} = \frac{e}{h} \int dE \{[M_{Nh} - T_{Nh,Nh}] [f_0 (E + \mu_N) - f_0(E)] + [-T_{Nh,Ne}]$$

Using symmetry properties between electronic and hole terminals, namely $I_{Ne \leftarrow Ne}(E) = I_{Nh \leftarrow Nh}(-E)$ and $I_{Ne \leftarrow Nh}(E) = I_{Nh \leftarrow Ne}(-E)$, together with $f_0(E) = 1 - f_0(-E)$ we get for $I_N = I_{Ne} + I_{Nh}$:

$$I_N = \frac{2e}{h} \int dE [1 - T_{Ne,Ne} + T_{Nh,Ne}] [f_0 (E - \mu_N) - f_0(E)]$$

The term $T_{Nh,Ne}$ is responsible for Andreev reflection thereby causing an increase in the current, while the term $T_{Ne,Ne}$ represents normal reflection which decreases it. Linearizing the above equation for small voltages such that µN = qV , we get a conductance of $G = 4e^2/h$ per mode if we assume perfect Andreev reflection, signified by TNe,Nh = 1, as shown below. Thus an N-S

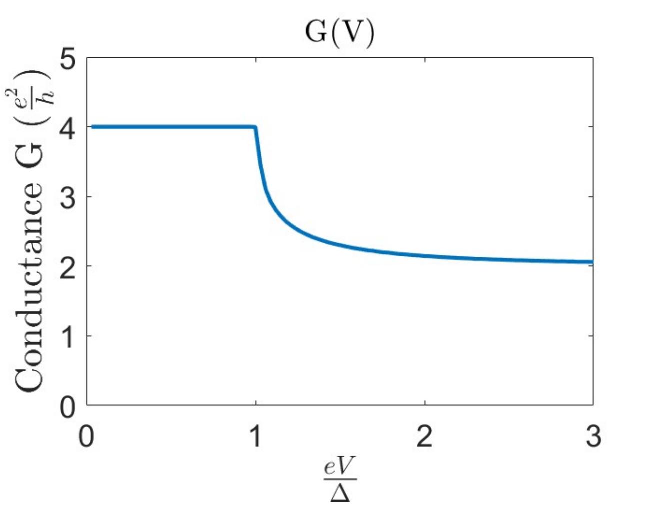

Figure 4: Conductance for a SN junction at low temperature as a function of bias

structure which has perfect Andreev reflection at the superconducting side faces contact resistance only near the metallic constriction. Thus, the chemical potential of the +k states in the normal side follows that of electrons and that of -k states follows that of holes in the normal side.

C. Green's Function

We use the tight-binding model with the BdG equation for a NS interface with $\Delta = 0$ for normal metal, and finite Δ for superconducting side.

$$[H]_{BdG} = \begin{pmatrix} \alpha & \beta & 0 & 0 \\ \beta^\dagger & \alpha & \beta & 0 \\ 0 & \beta^\dagger & \alpha & \beta \\ . & . & . & . \end{pmatrix}$$
$$[\alpha] = \begin{pmatrix} \epsilon-\mu & \Delta \\ \Delta^* & -(\epsilon-\mu) \end{pmatrix} \tag{6}$$
$$[\beta] = \begin{pmatrix} -t & 0 \\ 0 & t \end{pmatrix}$$

The Green's function is given by

$$G^r(E) = \left[EI - H_{BdG} + i\eta\right]^{-1}. \tag{7}$$

$$G^r(E) = \left[(E+i\eta)I - H - \Sigma_L - \Sigma_R\right]^{-1} \tag{8}$$

where the lead self energies are given via the surface Green's function $g_{sL,sR}$ as $\Sigma_L(E) = \beta^\dagger g_{sL}\beta$ and $\Sigma_R(E) = \beta g_{sR}\beta^\dagger$ with $g_{sL,sR}$ satisfying a recursive relation to be solved iteratively as

$$g_{sL}(E) = \left[EI - \alpha_S - \beta^\dagger g_{sL}\beta\right]^{-1}$$
$$g_{sR}(E) = \left[EI - \alpha_S - \beta g_{sL}\beta^\dagger\right]^{-1}..$$

The term $g_{sL,sR}$ is evaluated on the plane defining the surface at the lead-channel interface with the onsite matrix on the surface plane α_S.

For calculations of dc quantities, we have a common gauge transformation that keeps the superconductors at $\mu = 0$. However, no common gauge transformation is possible for a SNS junction and non-equilibrium BdG equation is used.

NS Junction

The Retarted Green's function is given by:

$$G^n(E) = G^r(E)\left(\Gamma_L(E) + \Gamma_R(E)\right)G^{r\dagger}(E)$$

The quantities $\Gamma_{L,R}(E)$ represent the in-scattering functions from leads L and R respectively evaluated in the gauge transformed energy domain as

$$\Gamma_{L,R}(E) = i\left[\Sigma_{L,R}(E) - \Sigma^\dagger_{L,R}(E)\right] f_{L,R}(E)$$

where the contact self energies $\Sigma_{L,R}(E)$. In this formulation, all different components of the currents can then be deduced from the current operator

$$I_{op} = \frac{e}{h}\left[H_{i,i\pm1}G^n(i\pm1,i) - G^n(i,i\pm1)H_{i\pm1,i}\right],$$

where the $H_{i,i\pm1}$ term represents the hopping part of the Hamiltonian in BdG space.

D. DC Josephson Effect and QP Tunneling

We will begin by examining a basic tunnel junction consisting of two superconducting contacts. Using the transfer matrix approach, we observe that tunneling is described by a matrix element M, which we assume is not dependent on energy. Under this assumption, the device region being examined consists of just two points, representing the edge sites of each contact. Our approach involves conducting a first-order calculation (with respect to M) of the tunneling currents. The system's retarded Green's function matrix is expressed as:

$$[G] = \begin{pmatrix} (g_{sL})^{-1} & -M \\ -M^\dagger & (g_{sR})^{-1} \end{pmatrix}^{-1} \tag{9}$$

where $g_{sL(R)}$ denote the surface Green's function associated with the left (right) contact. To first order, we can expand the above equation as

$$[G] \approx \begin{pmatrix} g_{sL} & g_{sL}Mg_{sR} \\ g_{sR}M^\dagger g_{sL} & g_{sR} \end{pmatrix}$$

$$g_{sL,R} = \begin{pmatrix} g^{ee}_{sL,R} & g^{eh}_{sL,R} \\ g^{he}_{sL,R} & g^{hh}_{sL,R} \end{pmatrix} \tag{10}$$

evaluate the electron correlators G^nas

$$G^n = G^R\begin{pmatrix} \gamma_L & 0 \\ 0 & \gamma_R \end{pmatrix}G^\dagger$$

where $\gamma_{L,R} = i\left(\sigma_{L,R} - \sigma^\dagger_{L,R}\right)f_{L,R}(E)$ is the inscattering function associated with each electrode. The current operator in our case, where $H_{j,j\pm1} = M$ is:

$$\begin{aligned} I_{OP} &= \frac{e}{h}\left[\left(Mg_{sR}M^\dagger\alpha_L + M\alpha_R M^\dagger g_{sR}\right.\right. \\ &\left.\left.-M^\dagger\alpha_L M g^\dagger_{sR} - M^\dagger g_{sL}M\alpha_R\right)\right] \\ &= \frac{e}{h}|M|^2\left[\left(\tau_3 g_{sR} tau_3\alpha_L + \tau_3\alpha_R\tau_3 g_{sL}\right.\right. \\ &\left.\left.-\tau_3\alpha_L\tau_3 g^\dagger_{sR} - \tau_3 g_{sL}\tau\alpha_R\right)\right], \end{aligned}$$

where $\tau_3 = \begin{pmatrix} 1 & 0 \\ 0 & -1 \end{pmatrix}$ and $\alpha_{L,R} = g_{sL,R}\sigma^<_L g^\dagger_{sL,R} = \alpha^\dagger_{L,R}$. From the above expression we can derive the expression for the total dc current in the form $I(V) = \int dE|M|^2 i_0(E,V)$, where $i_0 = i_J + i_{QP}$, with i_J being the Josephson current at zero bias and i_{QP} is the quasiparticle current that appears with a voltage bias. The expressions for i_J and ${}^iQP$ are given as

$$\begin{aligned} i_J(E) &= 4Re\left[g^{he}_{sL}(E)g^{ch}_{sR}(E) - g^{hc}_{sR}(E)g^{eh}_{sL}(E)\right]f(E) \\ i_{QP}(E) &= \left[a^{ce}_R(E+V)a^{cc}_L(E) + a^{hh}_R(E+V)a^{hh}_L(E)\right] \\ &\qquad\times\left[f(E) - f(E+V)\right] \end{aligned}$$

II. RESULTS

A. Density of States in a superconductor

```
% DOS for a superconducting contact using the
surface Green's function i.e local DOS at the
interface

% t0 : tight binding parameter = hbar^2/(2 m a^2)
% t0 units : eV
t0 = 1.0;

% kT : k_B * Temperature(K)
% kT units : eV
% kT default value : 0.026 eV (Room temperature)
kT = 0.0001;

alpha = [2*t0 + mu  0;0 -2*t0 - mu];
beta = -t0* [1 0; 0 -1];

% local density of states
a = zeros(1,length(E_vec));

% electron and hole density
n = zeros(1,length(E_vec));

for ii = 1:length(E_vec)
    E = E_vec(ii);

    g = surface_g_f(E,alpha,beta);
    A = 1j*(g - g');

    fermi = 1.0/(1.0 + exp((E - mu)/kT));
    Fermi = [fermi(E,-mu,kT) 0;0 1-fermi(E,mu,kT)];

    N = A * Fermi;
    a(ii) = trace(A);
    n(ii) = trace(N);
end
```

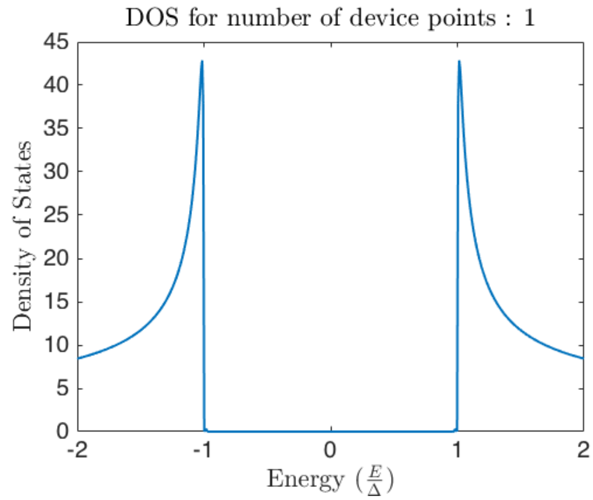

Figure 5: DOS for a superconducting contact

1. *Current-Phase Relation*

```
    %Transfer Matrix
M=0.095

%energies in eV
t0 = 0.1;
Delta = 0.008;
kT = 0.002;

phi_vec = 0:0.1:2*pi;
I_phi = zeros(1,length(phi_vec));

for jj = 1:length(phi_vec)
    phi = phi_vec(jj);

    Delta1 = Delta;
    alpha1 = [2*t0 Delta1; conj(Delta1) -2*t0];
    beta1 = -t0* [1 0; 0 -1];

    Delta2 = Delta * exp(1i*phi);
    alpha2 = [2*t0 Delta2; conj(Delta2) -2*t0];
    beta2 = -t0* [1 0; 0 -1];

    for ii = 1:length(E)
        EE = E(ii);

        %calculation of g iteratively
        g1 = inv((EE + 1i*eta)*eye(2) - alpha1
        - beta1'*g1*beta1);
        g2 = inv((EE + 1i*eta)*eye(2) - alpha2
        - beta2'*g2*beta2);

        I_J(ii) = 4 * real(g1(2,1)*g2(1,2) -
        g2(2,1)*g1(1,2)) * 1.0/(1 + exp(EE/kT));
    end
    I_phi(jj) = sum(I_J);
end
```

B. Point SNS Junction

sNS junction has a current phase relationship due to the form of the bulk SC wavefunction and schrodinger equation.

Josephson Equations

$$I(\phi(t)) = I_c \sin\phi(t) \tag{11}$$

$$\frac{\partial\phi}{\partial t} = \frac{2eV(t)}{\hbar} \tag{12}$$

The second equation is used to study AC josephson effects while the first gives us DC Josephson effect.

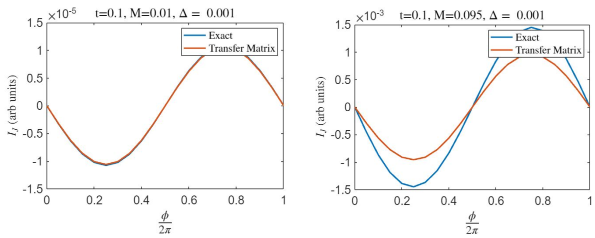

(a)$M \ll \Delta$ (b)$M \sim \Delta$

Figure 6: Comparison of exact v/s approximate($M \ll \Delta$) calculation of current-phase relationship for a point SNS Junction.

2. Long N, Density of States: Andreev Bound States

```
% DOS calculation including Andreev bound states

% number of points in the device (channel)
N_D = 100;

% t0 : tight binding parameter = hbar^2/(2 m a^2)
% t0 units : eV
t0 = 1;

% Device Hamiltonian (BdG)
% mu = 0 and Delta = 0 in the device region

alpha = [2*t0  0; 0 -2*t0];
beta = -t0* [1 0; 0 -1];
```

$$[H]_D = \begin{pmatrix} \alpha & \beta & 0 & 0 \\ \beta^\dagger & \alpha & \beta & 0 \\ 0 & \beta^\dagger & \alpha & \beta \\ . & . & . & . \end{pmatrix} \tag{13}$$

```
% Delta: Superconducting order paramter
% Delta units : eV
Delta = 0.01;

% mu1 : electrochemical potential of the
left contact
mu1 = 0.0;
% mu2 : electrochemical potential of the
right contact
mu2 = 0.0;

% phi : phase difference between the two
superconductors
phi = 0;

Delta1 = Delta;

Delta2 = Delta * exp(1j*phi);

for ii = 1:length(E_vec)
```

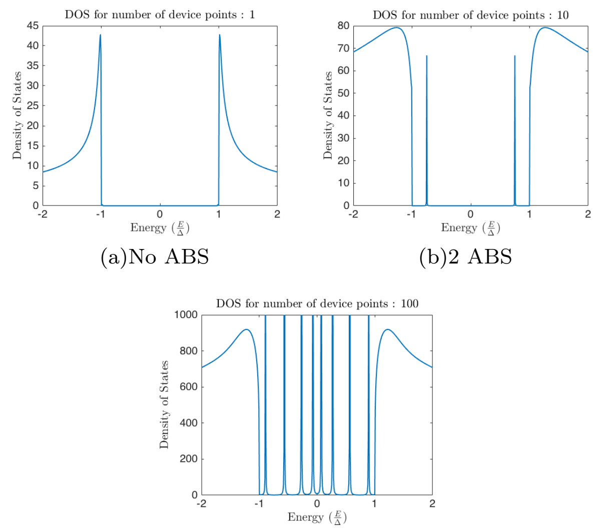

(a)No ABS (b)2 ABS

(c)Multiple ABS

Figure 7: The ABS occur due to phase matching possible in ¿1 point N regions in a SNS junction.

```
    E = E_vec(ii);

    g1 = surface_g(E,alpha1,beta1,eta);
    g2 = surface_g(E,alpha2,beta2,eta);

    Sigma1 = zeros(2*N_D);
    Sigma1(1,1) = g1(1,1);
    Sigma1(1,2) = g1(1,2);
    Sigma1(2,1) = g1(2,1);
    Sigma1(2,2) = g1(2,2);

    Sigma2 = zeros(2*N_D);
    Sigma2(2*N_D - 1,2*N_D - 1) = g2(1,1);
    Sigma2(2*N_D - 1,2*N_D) = g2(1,2);
    Sigma2(2*N_D,2*N_D - 1) = g2(2,1);
    Sigma2(2*N_D,2*N_D) = g2(2,2);

    G_D = inv((E + 1i*eta) .* eye(2*N_D) - H_D
    - Sigma1 - Sigma2);

    A(ii) = trace(1j * (G_D - G_D'));
end
```

3. Current-Voltage Relationship

```
    %energies in eV
t0 = 0.1;
Delta = 0.008;
Delta2=2*Delta1

kT = 0.01;
phi = 0.2*pi;
```

```
mu = 0;

for ii = 1:length(V_vec2)
    V = V_vec2(ii);

    Delta1 = Delta;
    alpha1 = [2*t0-mu Delta1; conj(Delta1) -2*t0+mu
    beta1 = t0* [1 0; 0 -1];

    Delta2 = fac * Delta * exp(1i*phi);
    alpha2 = [2*t0-mu Delta2; conj(Delta2) -2*t0+mu
    beta2 = t0* [1 0; 0 -1];

    for jj = 1:length(E)
        EE = E(jj);

        %calculation of g iteratively
            g1 = inv((EE + 1i*eta)*eye(2) - alpha1
            - beta1'*g1*beta1);
        %calculate g2 for E = E + V
            g2 = inv((EE + V + 1i*eta)*eye(2) -
            alpha2 - beta2*g2*beta2');
        a1 = 1i * (g1 - g1');
        a2 = 1i * (g2 - g2');

        I_E(jj) = (a2(1,1) * a1(1,1) + a2(2,2)*a1(2,2)) * (1.0/(1 + exp((EE)/kT))
        - 1.0/(1 + exp((EE+V)/kT)));
    end
    I_V2(ii) = sum(I_E);
end
```

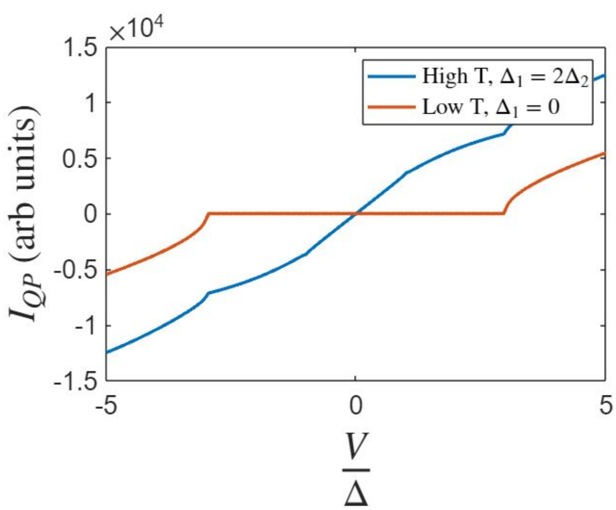

Figure 8: I-V Curve for a SNS junction and SN Junction, also showing temperature dependence

III. IMPORTANT WORKS

The study of Josephson junctions has been a rich area of research for several decades, with many important works and discoveries along the way. Some of the key contributions to the field are:

- The discovery of the Josephson effect: In 1962, Brian Josephson predicted that two superconductors separated by a thin insulating barrier could exhibit a non-linear current-voltage relationship, which is now known as the Josephson effect. This effect has since been experimentally observed and is the basis for many Josephson junction applications.

- The development of the SQUID: The Superconducting Quantum Interference Device (SQUID) was developed in the 1960s and is based on the Josephson effect. SQUIDs are extremely sensitive detectors of magnetic fields and have applications in a variety of fields, including medical imaging and materials science.

- The discovery of the fractional Josephson effect: In 1988, researchers discovered that a Josephson junction could exhibit a current-voltage relationship that was not an integer multiple of the Josephson constant. This discovery led to a better understanding of the quantum behavior of superconductors.

- The development of superconducting qubits: Superconducting qubits are the basis for many quantum computing applications, and Josephson junctions are a key component of these devices. In the

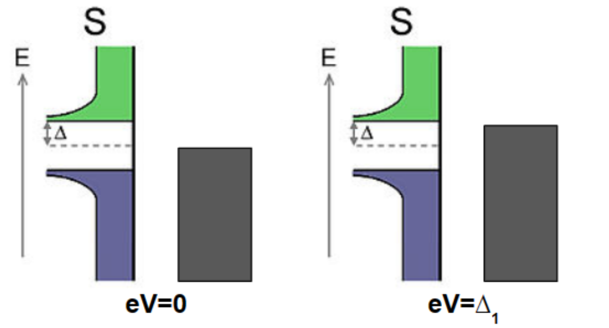

Figure 9: NS Junction, how energy levels shift with potential

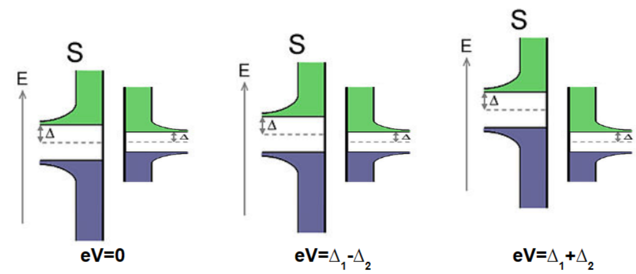

Figure 10: SNS Junction, how energy levels shift with potential

1990s, researchers demonstrated the first working superconducting qubits, and since then, many advancements have been made in this area.

- The development of high-temperature superconductors: In the 1980s, researchers discovered a class of materials that exhibited superconductivity at much higher temperatures than previously thought possible. Josephson junctions have been used to study the properties of these materials and to develop new applications based on their unique properties.

IV. CURRENT STATUS AND APPLICATIONS

Josephson junctions have been the subject of extensive research and development over the past few decades, and have found a variety of applications in both fundamental research and technological applications. Some of the current status and applications of Josephson junctions are discussed below:

- Quantum Computing: Josephson junctions have become a key component in the development of quantum computers, which offer a significant speedup over classical computers for certain types of problems. The superconducting qubits used in many quantum computers are based on Josephson junctions, and researchers are working on scaling up these devices to create large-scale quantum computers.
- Metrology: Josephson junctions are used in a variety of high-precision measurement applications, including voltage standards and current standards. The Josephson voltage standard is used to define the volt, the SI unit of electric potential, with extremely high accuracy.
- Sensors: Josephson junctions can be used as extremely sensitive detectors for a variety of physical quantities, such as magnetic fields and radiation. These sensors are used in a variety of applications, including medical imaging and materials analysis.
- Microwave Generation and Detection: Josephson junctions can be used to generate and detect microwave radiation with very high precision. This is useful in a variety of applications, including telecommunications and radio astronomy.
- Superconducting Electronics: Josephson junctions are used in the development of superconducting electronics, which operate at extremely low temperatures and offer very low power consumption. These devices have potential applications in high-speed computing and data processing.

V. CONCLUSION

The Non-equilibrium Green's Function (NEGF) formalism is a powerful tool in the study of electronic transport in mesoscopic systems, including Josephson junctions. Josephson junctions are a type of superconducting device that exhibit a unique non-linear current-voltage relationship and have been extensively used in a variety of applications, including quantum computing and metrology.

The NEGF formalism is used to study the transport properties of Josephson junctions by considering the junction as a scattering problem, where electrons are injected from one electrode into the junction and then transmitted or reflected to the other electrode. The NEGF approach is particularly useful in studying the behavior of electrons in mesoscopic systems, where quantum effects play a significant role and classical descriptions are inadequate.

The NEGF approach provides a framework for calculating the current-voltage characteristics of Josephson junctions, as well as other transport properties, such as conductance and shot noise. By modeling the scattering properties of the junction using NEGF, researchers can investigate the effects of different parameters on the transport properties, such as the strength of the coupling between the electrodes and the degree of coherence of the superconducting phase.

In summary, the NEGF formalism is an essential tool in the study of Josephson junctions and other mesoscopic systems, providing a powerful framework for investigating the transport properties of these systems and shedding light on the fundamental physics underlying their behavior.

Acknowlegements: I would like to thank Prof. Bhaskaran Muralidharan for guidance and discussions. I would also like to thank the teaching assistants, Mr. Shlok Vaibhav Singh and Mr. Venkatesh Vadde for the discussions.

VI. REFERENCES

- Supriyo Datta et. al., "Scattering Theory of Transport for Mesoscopic Superconductors
- https://doi.org/10.1017/CBO9781139020916.016, " Superconductivity and BCS Theory".
- R. M. Fernandes, BCS Theory of Superconductivity
- Current-voltage relation for asymmetric ballistic superconducting junctions, Magnus Hurd, Supriyo Datta, and Philip F. Bagwell

– Ballistic Josephson-current flow through an asymmetric superconductor - normal metal - superconductor junction Li-Fu Chang and Philip F. Bagwell

– Lessons from Nanoelectronics, Suppriyo Datta, https://doi.org/10.1142/10440

– Quantum Transport - Atom to Transistor, Suppriyo Datta

Appendix A: Particle-Hole Symmetry

Particle-hole symmetry is a fundamental concept in condensed matter physics that refers to a type of symmetry between the addition of a particle and the removal of a hole in a material. Specifically, it is a symmetry between the creation of an electron in a system and the removal of an electron from the same system, leaving behind a hole.

Under particle-hole symmetry, the energy spectrum of a material remains unchanged when the energy of each state is inverted around a specific energy value called the Fermi energy. This means that for every energy level above the Fermi energy in the system with particles, there exists a corresponding energy level below the Fermi energy in the system without particles, and vice versa.

Up-spin electrons $\mathrm{Hu}' = \mathrm{i}\hbar\frac{\partial \mathrm{u}'}{\partial \mathrm{t}}$

Down-spin holes

$$-H^{*}\mathrm{v}' = \mathrm{i}\hbar\frac{\partial \mathrm{v}'}{\partial \mathrm{t}}$$

* utkarshsaxena2302@gmail.com